Shape of the surface of a liquid under indentation by a flat punch -effect of surface tension for a semi-infinite axisymmetric media in the presence of gravity

Christophe Fond

Shape of the surface of a liquid under indentation by a flat punch - effect of surface tension for a semi-infinite axisymmetric media in the presence of gravity

Christophe Fond

Laboratoire ICube, 2 rue Boussingault, F67000 Strasbourg

Résumé

The contact between a cylindrical flat indenter and an incompressible, non-viscous liquid is considered. The behaviour is totally controlled by the assumed constant surface tension and gravity. An analytical approach and a numerical solution are developed to describe the shape of the surface as a function of the applied force. In the absence of an exact solution, an approximate solution is proposed.

Keywords: nanomechanics, indentation, surface tension, contact, liquid, incompressible, gravity

1. Preamble

This article follows two articles, in English and French, concerning the indentation of an elastic medium for which surface tension acts considerably. In the situation where the elasticity of the medium disappears in front of the surface tension, as is the case for microscopic indenters and compressible soft media, the problem tends towards the indentation of a stretched membrane (Fond, 2018c), (Fond, 2018d). In the situation where the medium is almost incompressible and very soft in shear, the problem tends towards that of a liquid. In finite medium the solutions are analyzed and it is shown in (Fond, 2018a) et (Fond, 2018b) that gravity can be neglected, always in the case of microscopic indenters. For semi-infinite environments, it will be shown further on that the effect of gravity can no longer be neglected. Considering a semi-infinite media and the attempt to superimpose the effects of the response of the bulk (Boussinesq, 1885) and that of the surface, it is

therefore necessary to know the solution for these two situations considered independently. It has been shown that the insertion of the punch into a liquid tends towards infinity when gravity is neglected. The aim here is to provide a suitable solution with consideration of gravity, a case that does not admit an analytical solution. Many articles have been dedicated to this subject of indentation, for example (Chakrabarti and Chaudhury, 2013), (Cortat and Miklavcic, 2003), (Cortat and Miklavcic, 2004), (Butt et al., 2005), (Colchero et al., 1998), (Cappella and Dietler, 1999), (Forcada et al., 1991), the article closest to the present analysis being that of (Chan et al., 2001).

2. Introduction

The liquid is supposed to be incompressible. The static situation is considered, i.e. there is no inertial effect. An established and stable state is considered so that the viscosity of the fluid is neglected. The surface tension γ, assumed constant, balances a local pressure $p-\rho g\delta$ exerted on the surface at a horizontal distance r from the center of the flat punch (Fond, 2018b). The static equation of equilibrium in Fig. 1 is therefore formulated by :

$$p-\rho g\delta=-\gamma(\frac{sin\ (atan\delta')}{r}+\frac{\delta"}{(1+\delta'^2)^{3/2}}) \tag{1}$$

where p is the pressure under the indenter, ρ the density of the liquid, g the acceleration of gravity and δ the height of the surface at the distance r. For a classic free surface problem, the maximum height $\delta_{asympt.}$ corresponds to an infinite radius from where $p=\rho g\delta_{asympt.}$. This equation can be rewritten $p-\rho g\delta=-\gamma(\frac{\delta'}{r\sqrt{1+\delta'^2}}+\frac{\delta'}{(1+\delta'^2)^{3/2}})$. For calculation convenience it was chosen $\delta=0$ at the base of the punch. If the zero height reference is the free surface then the punch base will be at the depth corresponding to $-\delta_{asympt.}$. This change of origin will lead to the depth $\delta(r)-\delta_{asympt.}$. The equilibrium of the flat punch is given by (see Fig. 2) :

$$F=2\pi af+\pi a^2p \tag{2}$$

where f denotes the Laplace's tension at the corner of the punch given by $f=\gamma sin(\beta(a))$.

3. Numerical integration of the equilibrium equation

Since the equilibrium equation 1 does not admit an analytical solution, a calculation by numerical integration has been developed. A distance must

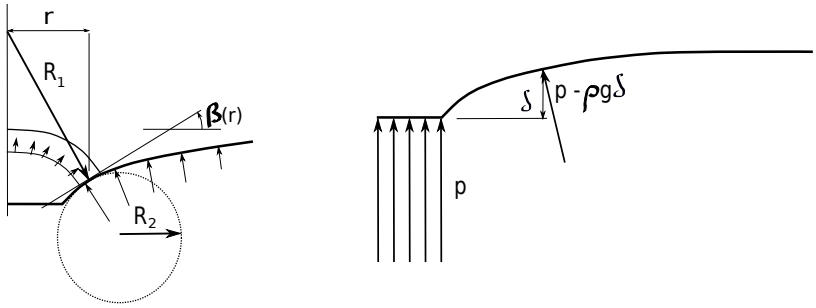

Figure 1: Pressures and curvatures for an axisymmetric model (left) and gravity-related pressure variation (right).

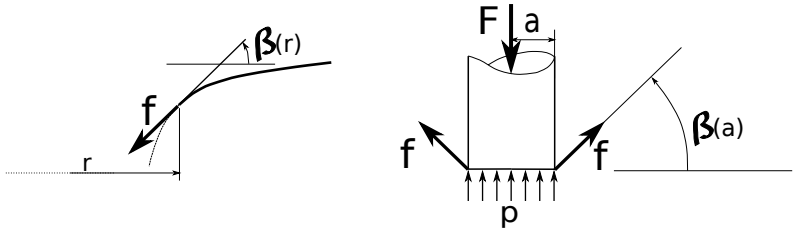

Figure 2: Laplace's tension (left) and flat punch equilibrium (right).

be chosen $D >> a$ that ensures to be on the numerical asymptote [1]. The line segment defined by the two points a and D at $z = 0$, i. e. $(a, 0) - (D, 0)$, is discretized into sub-segments $(r_i, 0) - (r_{i+1}, 0)$, i ranging from 0 to n with $r_0 = a$ and $r_n = D$. Noticing $b_a = log_{10}(a)$ and $b_D = log_{10}(D)$, the spatial discretization is done so that $r_i = 10^{b_a+(i/n)(b_D-b_a)}$. The surface is composed of line segments $(r_i, \delta_i) - (r_{i+1}, \delta_{i+1})$. Given an angle $\beta(a)$, the first segment is given by $(r_0, 0) - (r_1, \delta_1)$ where δ_1 denotes $(r_1 - a)(tan(\beta(a)))$. In order to know the following points (r_2, δ_2) then (r_i, δ_i) a dichotomy procedure looks for the value of δ_i which respects the equation. 1 with a precision based on the value $abs(\frac{\delta_i^m - \delta_i^{m-1}}{\delta_{i-1} - \delta_{i-2}})$ where m denotes the iteration by dichotomy to find δ_i. For the calculations presented here the precision chosen is 10^{-6} and $n = 1000$ for the number of segments. The curves δ' and δ" are calculated from the second degree polynomial which passes through the three points (r_i, δ_i), (r_{i+1}, δ_{i+1}) and $(r_{i+2}, \delta_{i+2}i + 2)$. The slope δ' is the slope of the polynomial

[1] for the results presented here in double precision, i. e. to the nearest 10^{-15}

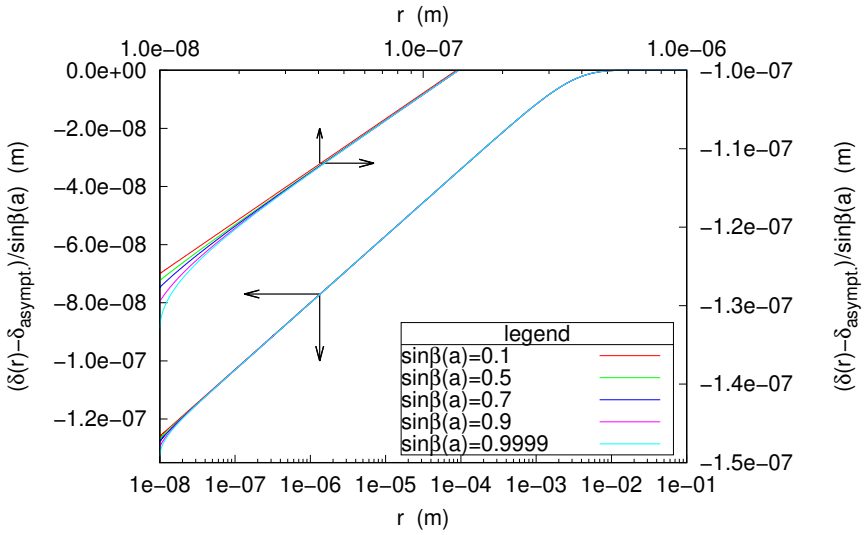

Figure 3: Normalized surface profiles for $\gamma = 0.07d/m^2$, $\rho = 1000kg/m^3$, $g = 9.81m/s^2$, $a = 10nm$ and $sin\beta(a) = 0.1, 0.5, 07$ and 0.9. At the top left is a zoom on the fairly non-linear part for which typically $sin\beta(r) \not\approx \beta(r)$.

function in the middle of the segment.[2]

Whatever the force exerted on the object, as long as $\beta(a) < \pi/2$ [3], the surface disturbance is typically exerted at a distance of $1cm$ as shown in Fig. 3 for $\gamma = 0.07d/m^2$, $\rho = 1000kg/m^3$, $g = 9.81m/s^2$, $a = 10nm$. For values of r large enough that $sin\beta(r) \approx sin\beta(r)$ we find the values predicted by the approximate analytical solutions and the curves normalized by $sin\beta(a)$[4] are superimposed.

Fig. 4 shows that the reaction force to indentation varies almost linearly with the indentation depth. Indeed, less than 6% error is made on the prediction of force by considering that the original slope is kept up to

[2]The procedure can also do the "reverse path" from D to a from a perturbation defined in D by (r_n, δ_n) and (r_{n-1}, δ_{n-1}) but in this direction it is not possible to predict a priori $sin\beta(a)$.

[3]for $\beta(a) \to \pi/2$, the contribution of surface tension can no longer increase and the object would sink into the liquid until the pressure under the punch can balance the force exerted. This situation is discussed below.

[4]remind us that normalizing by $sin\beta(a)$ amounts to normalizing by the applied force since the contribution of surface tension to equilibrium is $f = 2\pi\gamma sin\beta(a)$ and that $F \approx f$ if $\pi a^2 p << f$.

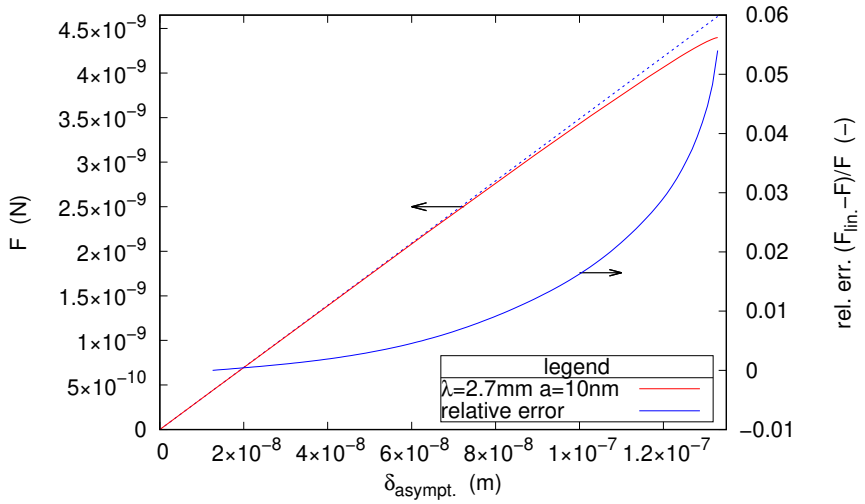

Figure 4: Force versus indentation depth for $\gamma = 0.07d/m^2$, $\rho = 1000kg/m^3$, $g = 9.81m/s^2$, $a = 10nm$. The dotted line shows the slope at the origin. The relative error is calculated with the values of this line.

$sin\beta(a) = 0.9999$, i. e.$\beta(a) = \pi/2.02$. For the parameters chosen for the illustration, the contribution of hydrostatic pressure under the punch, term $\pi to^2 p$ of the equation 2 where $p = \rho g \delta_{asympt.}$, is negligible.

A dimensional analysis allows to adimension by introducing the capillary length $\lambda = \sqrt{\frac{\gamma}{\rho g}}$ (see Appendix A). The Fig. 5 provides the results of the numerical integration described above for $sin\beta(a) = 0.5$ [5]. Around $r = \lambda$ the effect of gravity is felt and it goes from a trend $\delta(r) = asin\beta(a)log(r/a)$ to the asymptote $\delta \approx 0$ for $r > \frac{6}{5}\lambda$. Whatever the force exerted on the object, the surface disturbance is typically less than 10λ.

For the intended use, essentially the maximum depression is sought. From the previous equations it comes:

$$\delta_{asympt.} \approx a\ sin\beta(a)\ log(6\lambda/5a) \tag{3}$$

or even:

$$\delta_{asympt.} \approx \frac{F}{2\pi\gamma}\ log(6\lambda/5a) \tag{4}$$

[5] the maximum force will be reached for $sin\beta(a) \to 1$

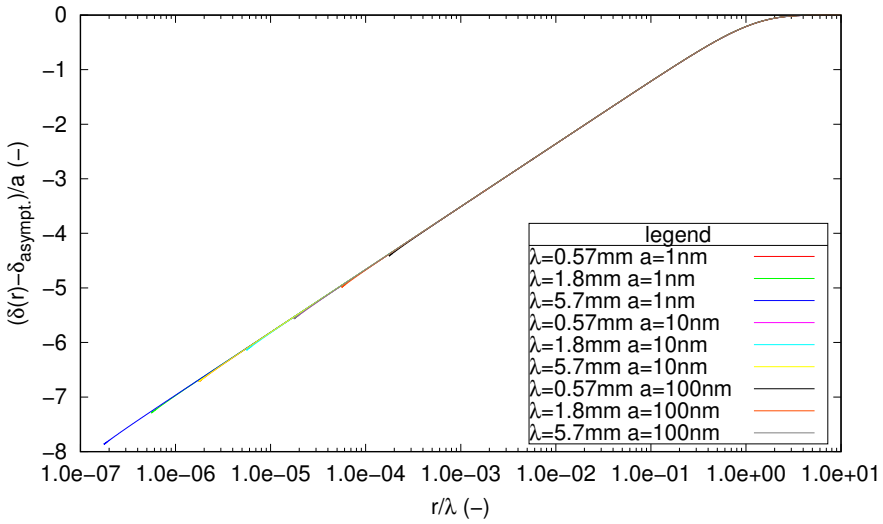

Figure 5: Results of numerical integration and normalization by $\lambda = \sqrt{\frac{\gamma}{\rho g}}$: indentation depth $(\delta(r) - \delta_{asympt.})$ as a function of distance r for $sin\beta(a) = 0.5$.

so that:

$$\delta_{asympt.\ max} < a\ log(6\lambda/5a) \tag{5}$$

for a microscopic flat punch floating on a liquid of similar property to water on earth, the contribution to the pressure balance under the punch is always negligible compared to the contribution of surface tension.

3.1. Approximative function

The analysis of the solutions of the second order differential equation in Annex Appendix A provides information to find a suitable approximate function. In addition, a dimensional analysis highlights the term $\sqrt{\frac{\rho g}{\gamma}}$ commonly referred to as capillary length. For the intended use, essentially the maximum depression is sought and a slight error in the shape of the surface will be tolerated.

$$\delta(r) \approx asin\beta(a)\frac{2e^{-r/\Lambda}}{1+e^{-r/\Lambda}}log(r/\Lambda) \tag{6}$$

où $\Lambda \approx \frac{6}{5}\sqrt{\frac{\gamma}{\rho g}}$. Rappelons que $F = 2\pi\gamma a\ sin\beta(a)$. The approximate function given by the eq. 6 and illustrated in Fig. 6 shows an underestimation of the

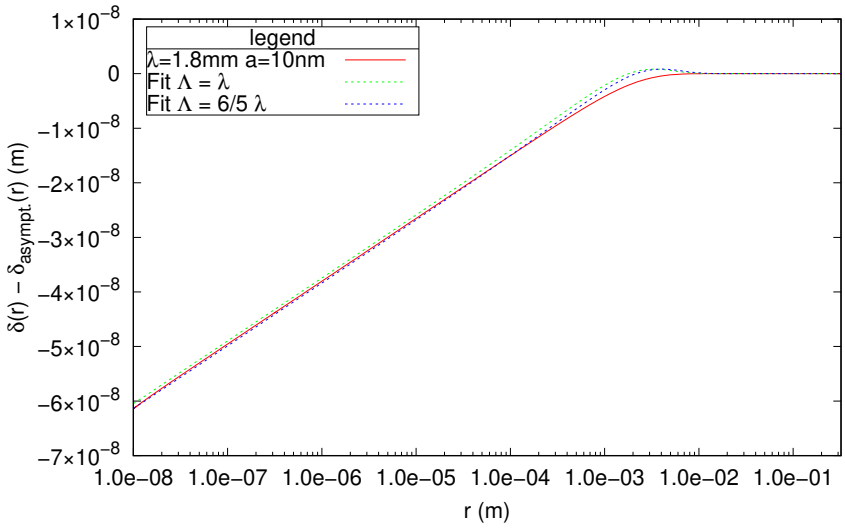

Figure 6: Approximate function to describe the indentation depth $-\delta$ as a function of distance r for $sin\beta(a) = 0.5$ and $\lambda = 1.8mm$.

sink in the vicinity of the asymptotic value and it should be considered that the depth $-\delta(r) < 0 \ \ \forall r$. Note that Λ should be chosen slightly higher than λ for a better approximation.

3.2. Case $\beta = \pi/2$

3.2.1. Non-submerged object

Fig. 7 illustrates the limit case for the angle at the corner of the punch. Let's first consider the case where no part is submerged, i.e. $\delta_{imm.} = 0$. When $\beta = \pi/2$, the contribution to the equilibrium of the surface tension is saturated and is worth $f = 2\pi a\gamma$. One of the two radii of curvature is exactly a, the other is at least a if $p \geq 0$. If the pressure p under the flat punch is negligible then the sum of the curves must cancel each other out. Hence, the two radii of curvature are worth a. For the above numerical calculations for which the object is microscopic, i.e. $a << \lambda$, and $sin\beta = 0.9999$, a simple geometrical calculation shows that the difference for $\delta_{asympt.}$ to the $sin\beta = 1$ situation is about $0.014a$. In view of the results shown in Fig. 5, this value appears negligible.

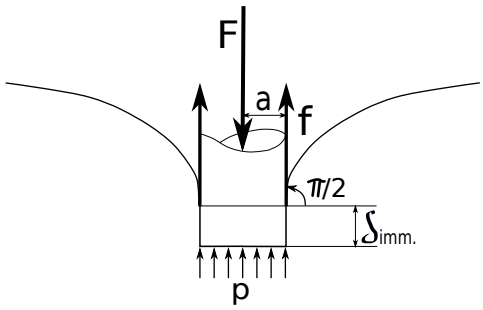

Figure 7: Flat punch equilibrium.

3.2.2. Submerged object

When $\delta_{imm.} > 0$, if the object has been immersed monotonously I assume that $\beta(a) = \pi/2$, then the maximum force that can be balanced is worth:

$$F = 2\pi a\gamma + \pi a^2 \rho g(\delta_{asympt.} + \delta_{imm.}) \tag{7}$$

At the limit of immersion, using the eq. 5 valid for typically $a < \frac{\lambda}{10}$, we get:

$$F = 2\pi a\gamma + \pi a^3 \rho g log(6\lambda/5a) \tag{8}$$

Fig. 8 is a numerical computation for microscopic objects such as $a < \lambda$ for water at room temperature, i. e. $\rho = 1000kg/m^3$, $g = 9.81m/s^2$ and $\gamma = 0.07$ hence $\lambda = 2.67mm$. It is clear that the contribution of the pressure under the punch is always negligible compared to that of the surface tension. On the other hand, the pressure related to gravity is used to calculate $\delta_{asympt.}$ and renders finite the depth considering an infinitely large liquid surface.

3.3. Objects with a size greater than the capillary length λ

The objective was achieved for objects of microscopic size for values of ρg typically in the order of $10^{+4}Pa$ and surface tensions typically in the order of 5 $10^{-2}N/m$. Nevertheless, for a better understanding let's analyze the situation where the object has a dimension greater than λ. It is obvious that the approximate solution provided in eq. 6 can no longer be satisfactory for objects larger than λ. Let's illustrate this situation in cases where $\rho = 10^{+3}kg/m^3$, $g = 9.81m/s^2$ and $\gamma = 0.07N/m$[6], i. e. $\lambda = 2.67mm$ for $a =$

[6]typically the case of water at room temperature on earth

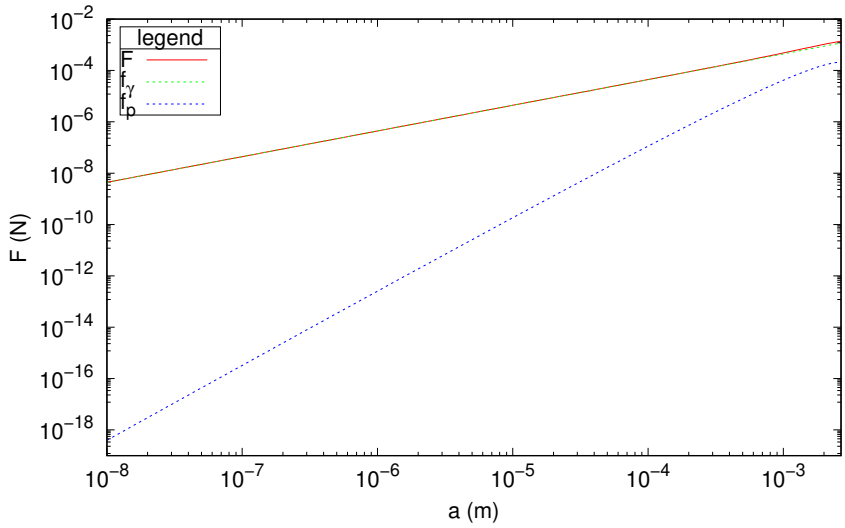

Figure 8: Reaction force versus punch radius. The dotted lines indicate the contributions of surface tension and pressure under the punch.

$8mm \approx 3\lambda$ and $a = 1dm \approx 37\lambda$ in Fig. 9. To ensure proper integration of the differential equation, an angle of $\beta(D)$ to the horizontal, very small, i. e. $\beta(D) << 1$, is given at a distance of D far enough from the edge of the punch, located at $r = a$, to be considered on the horizontal asymptote. Given this perturbation, integration is processed from D to a. When the depth $\delta(a)$ and the angle $\beta(a)$ have been determined by this way, the integration from a to D is performed and it is checked that the same surface profile is restored in both directions of integration. For the examples in Fig. 9, the perturbation was chosen so that the slope at the edge of the flat punch is maximum, i. e. $sin\beta(a) = 1$. Note that the force and depression increase almost linearly with this perturbation angle $\beta(D)$.

We notice in Fig. 9 that the disturbance length of the surface [7] is about λ from the punch edge. The contribution of the hydrostatic pressure below the punch surface to the total reaction force is about 64% for $a = 8mm$ and 96% for $a = 1dm$. It has been shown previously that this is negligible for microscopic[8] but in these cases it is considerable. The capillary length λ for the a radius therefore marks the transition between the sustentation by the

[7] length from the punch to find a nearly horizontal surface

[8] objects whose order of magnitude is much smaller than the order of magnitude of λ

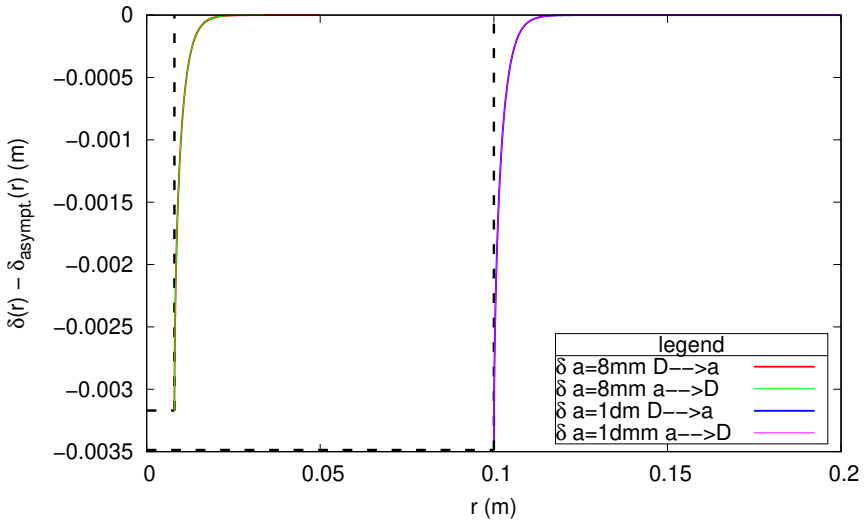

Figure 9: Surface profiles for $a = 8mm$ and $a = 1dm$ corresponding to $\lambda = 2.67mm$. The punches are materialized by the black dotted lines.

surface tension and the sustentation by the hydrostatic pressure generated under the tip by its depth. When $\beta(a)$ has reached $\pi/2$, if the punch continues to sink the "triple point" moves along the punch wall and the object floats or sinks.

4. Discussion

The aim was to provide a simple solution for the case of indentation of a flat punch in a semi-infinite planar medium, in the case where the mechanical behaviour of this medium is similar to that of a liquid. The medium is considered to be liquid, of negligible viscosity and incompressible. Calculations confirm that the latter assumption is appropriate. Indeed, the extremely small pressure variations are not likely to considerably change the density of the liquid whose compressibility is typically in the order of $2GPa$. The results provided here can be easily used and adapted for spherical or conical indenters for which the angle $\beta(a)$ will be limited by the geometry of the indentor. Indeed, since it has been shown here that for microscopic objects the contribution of pressure under the indent to equilibrium is a second order term, it will not be necessary to redeploy numerical integrations in these cases. Only objects with a capillary length greater than λ would require a

more precise quantification, but this does not concern the purpose of this article.

5. Conclusion

The calculations presented in this article for a liquid are consistent with those of (Fond, 2018c), (Fond, 2018a) for highly stressed membranes. They make it possible to locate the domain of validity in order to neglect certain parameters. They provide validation arguments for finite elements numerical indentation computations taking into consideration surface tension as well as elasticity for microscopic indentation. Given the relatively large volume of information required to properly present this numerical model, it will be presented in a separate article. This finite element numerical model calculates the effects of elasticity and surface tension in a coupled manner by covering the entire range of the ratio $\frac{\gamma}{a\mu}$ where μ refers to the shear modulus of the solid. It was therefore essential to have solutions in cases where $\frac{\gamma}{a\mu} << 1$ and $\frac{\gamma}{a\mu} >> 1$.

Appendix A. Analyse des solutions de l'équation différentielle du second ordre

The equilibrium equation 1 does not admit an analytical solution if all its terms are non-zero. In order to find a suitable approximation of numerical solutions, it is convenient to analyze analytical solutions when certain terms of the equation of equilibrium vanish.

Appendix A.1. $\rho g = 0$

For small angles, i. e. $sin\beta(a) \approx \beta(a)$, when $\rho g = 0$, there is an analytical solution to the equilibrium equation. For $p = 0$ it is formulated by:

$$\delta(r) \approx \frac{F}{2\pi\gamma} log(r/a) \tag{A.1}$$

with $r \geq a$.

Appendix A.2. $\delta' = 0$

When $\delta' = 0$, there is an analytical solution to the equilibrium equation formulated by:

$$\delta(r) = c_1 e^{r/\sqrt{\frac{\gamma}{\rho g}}} + c_2 e^{-r/\sqrt{\frac{\gamma}{\rho g}}} \tag{A.2}$$

where c_1 and c_2 are constants.

Appendix A.3. $\delta" = 0$

When $\delta" = 0$, there is an analytical solution to the equilibrium equation formulated by:

$$\delta(r) = c_3 e^{r^2/\frac{2\gamma}{\rho g}} \tag{A.3}$$

where c_3 is a constant.

References

Boussinesq, J., 1885. Application des potentiels à l'étude de l'équilibre et du mouvement des solides élastiques. Gauthier-Villars.

Butt, H.J., Cappella, B., Kappl, M., 2005. Force measurements with the atomic force microscope: Technique, interpretation and applications. Surface Science Reports 59, 1 – 152.

Cappella, B., Dietler, G., 1999. Force-distance curves by atomic force microscopy. Surface Science Reports 34, 1 – 104.

Chakrabarti, A., Chaudhury, M.K., 2013. Direct measurement of the surface tension of a soft elastic hydrogel: Exploration of elastocapillary instability in adhesion. Langmuir 29, 6926–6935. PMID: 23659361. https://doi.org/10.1021/la401115j.

Chan, D., Dagastine, R., White, L., 2001. Forces between a rigid probe particle and a liquid interface: I. the repulsive case. Journal of Colloid and Interface Science 236, 141 – 154.

Colchero, J., Storch, A., Luna, M., Gomez Herrero, J., Baro, A.M., 1998. Observation of liquid neck formation with scanning force microscopy techniques. Langmuir 14, 2230–2234. https://doi.org/10.1021/la971150z.

Cortat, F.P.A., Miklavcic, S.J., 2003. How closely can a solid approach an air-water surface without becoming wet? Phys. Rev. E 68, 052601.

Cortat, F.P.A., Miklavcic, S.J., 2004. Using stable and unstable profiles to deduce deformation limits of the air-water interface. Langmuir 20, 3208–3220. PMID: 15875850. https://doi.org/10.1021/la035651y.

Fond, C., 2018a. Enfoncement d'un poinçon plat dans une membrane fortement précontrainte : solution analytique.

Fond, C., 2018b. Forme de la surface d'un liquide ou d'un solide se comportant quasiment comme un liquide sous l'action de l'indentation par un poinçon plat - effet de la tension de surface.

Fond, C., 2018c. Indentation of a highly prestressed membrane by a flat punch: analytical solution.

Fond, C., 2018d. The shape of the surface of a liquid or a solid that behaves almost like a liquid under the action of indentation by a flat punch - the effect of surface tension.

Forcada, M.L., Jakas, M.M., Gras-Marti, A., 1991. On liquid-film thickness measurements with the atomic-force microscope. The Journal of Chemical Physics 95, 706–708. https://doi.org/10.1063/1.461420.